Micromechanical voxel unit cell for strength analysis of fiber reinforced plastics

Gerald Ernst* Christian Hühne Raimund Rolfes
Institute for Structural Analysis†
Leibniz University of Hannover

Abstract

For the strength analysis of unidirectional laminae an unit cell approach is illustrated. The unit cell is modeled with an approximate voxel mesh instead of a conventional mesh. Strengths are determined with continuum damage mechanics. A fracture energy formulation is applied to alleviate mesh dependency in the softening behavior. For direct loads the unit cell shows good capabilities for the prediction of strengths.

1 Introduction

For stiffness of UD-laminae analytical unit cell calculations and rules of mixture are state of the art, see e.g. [1]. Strengths as input parameters for failure criteria nonetheless are mostly determined by testing.

For the prediction of stiffness of textile composites computations with finite element unit cells play a major role. In contrast to analytical methods they allow for consideration of the spatial fibre architecture. As in UD-laminae strengths are determined by testing. In contrast to UD-laminae, it is hardly possible to experimentally determine the through thickness properties of textile composites which can no longer be assumed to be equal to the in-plane properties orthogonal to the fibers. Therefore unit cell models are an attractive alternative.

A special unit cell approach based on voxel discretization and continuum damage mechanics is developed. For calibration purposes, this approach is applied to a single UD-lamina and compared with experimental results of the World-Wide Failure Exercise (WWFE) by Hinton et al. [3].

*Email: g.ernst@isd.uni-hannover.de
†Appelstraße 9a, 30167 Hannover, Germany

2 Computational model

In this article material properties of UD-lamina are computed with the mechanical model of an unit cell. Therefore the lamina is assumed to be arranged regularly, free of defects and residual thermal stresses. In the WWFE [3] material parameters for four UD-laminae are given. The Silenka E-Glass 1200 tex / MY750/HY917/DY063 epoxy prepreg is chosen for the unit cell analysis, see tables 1 and 2. In contrast, material parameters for textile composites are difficult to determine experimentally. Therefore this computational procedure shall be calibrated through the comparison with test results of UD-composites for further application to textile composites.

The applied material is a standard damage model from the finite element program ABAQUS/Explicit. In the WWFE the material behavior of the components is not specified in detail, only initial modulus, tensile failure strain, tensile and compressive strength are given, see table 1. Based on these parameters the applied material was approximated, see Fig. 1. The glass fibres are assumed to be isotropic and linear elastic. An elasto-plastic material combined with isotropic hardening and isotropic damage is used to model the nonlinear behavior and the failure of the epoxy matrix material. The damage evolution is defined in terms of the fracture energy dissipation G_f after Hillerborg [2]. The fracture energy is given by

$$G_f = \int_0^{\bar{u}_f^{pl}} \sigma_y \bar{u}^{pl} = \int_0^{\bar{u}_f^{pl}} L\sigma_y \bar{\varepsilon}^{pl} \tag{1}$$

where σ_y is the yield stress, $\bar{\varepsilon}^{pl}$ is the equivalent plastic strain, $\bar{u}^{pl}$ is the equivalent plastic displacement, i.e. the fracture work conjugate of the yield stress after onset of damage (work per unit area of the crack) and $\bar{u}_f^{pl}$ the equivalent plastic displacement at failure. L is a characteristic length at each integration point, in this case the cube root of the integration point volume. This characteristic length is introduced to eliminate mesh dependency of results. Since the characteristic length is equal for all directions, elements with large aspect ratios will have rather different behavior depending on the direction in which the crack occurs. Therefore the voxel approach has significant advantages over conventional meshing methods. In the present case the damage evolution is assumed to have a linear form which leads to an evolution of the damage variable

$$d = \frac{L\bar{\varepsilon}^{pl}}{\bar{u}_f^{pl}} = \frac{\bar{u}^{pl}}{\bar{u}_f^{pl}} \quad . \tag{2}$$

Where

$$\bar{u}_f^{pl} = \frac{2G_f}{\sigma_{y0}} \tag{3}$$

with σ_{y0} being the yield stress at damage initiation.

The fracture energy for mode I cracking is given in the WWFE for the unidirectional lamina as $G_f = 165\frac{\mathsf{J}}{\mathsf{m}^2}$. It is assumed that fibre breakage does not occur so that the fracture energy of the epoxy is equal to the fracture energy of the lamina.

The application of plastic deformations is physically not reasonable but has no negative consequences on the results in the present computations. A dynamic analysis is carried out to avoid

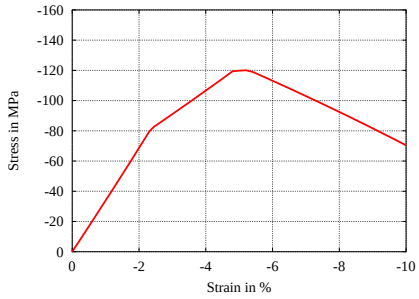

Figure 1: Material behavior

numerical instabilities after the onset of damage. An explicit time integration scheme is applied using the central-difference operator. A very small loading velocity is chosen so that the dynamic effects are negligible. Furthermore very small stiffness proportional damping is applied.

Fracture mechanics is an alternative approach, but requires an initial crack position. Such a position is not known therefore fracture mechanics is not considered for this problem.

2.1 Material Parameters

The material parameters shown in table 1 are taken from the WWFE [3]. The volume fraction of the lamina is given as $V_f = 60\%$.

Table 1: Mechanical properties of fibre and matrix

Properties	Unit	Silenka E-Glass 1200 tex	MY750/HY917/DY063 epoxy
Modulus	GPa	74	3.35
Strength	MPa	2150/1450[1]	80/120[1]
Failure strain	%	2.950/1.959[1]	5/–[1]
Shear Modulus	GPa	30.8	1.24
Poisson's ratio		0.2	0.35

[1] tensile/compressive

2.2 Discretization

The formation of fibres is far from being regular, for unit cells there are often two different approximations used: square and hexagonal arrangement, see Fig. 2. In Fig. 3 different discretization levels for square and hexagonal arrangements are shown. With the perspective of using the same model for textile composites volume elements are used and the mesh always is one element thick. Instead of a conformal mesh an approximate mesh is used. It does not attempt to exactly match the geometry of the unit cell, which is, by the way, only an assumption. The unit cell of an approximate mesh is subdivided in elements of the same size with an aspect ratio of unity, called "voxel"

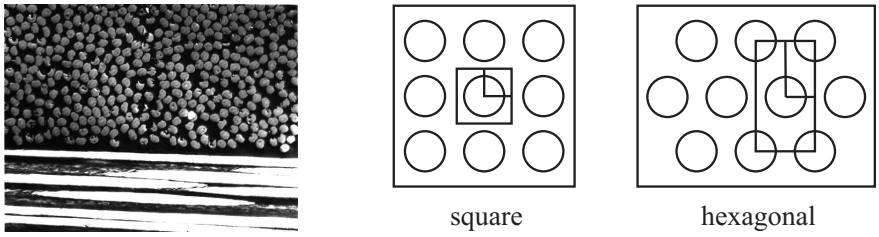

Figure 2: Micrograph (left) and assumed arrangement of fibres for unit cells

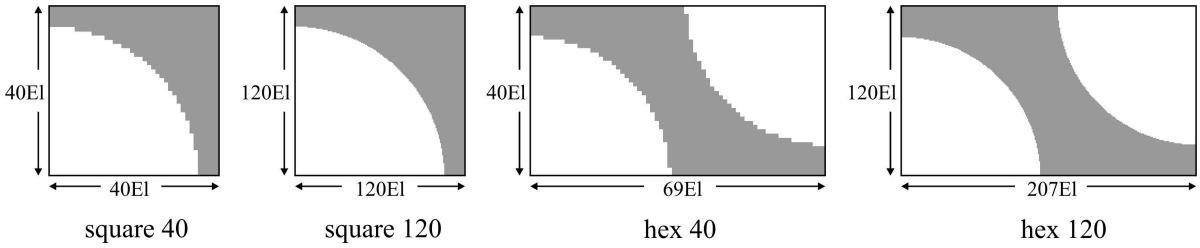

Figure 3: Discretization levels

(a volume pixel). The voxel approach has a number of advantages that mainly derive from the fact that especially with more complicated geometries many irregular elements appear in conformal meshes:

- Irregular elements have a negative influence on the performance and results of the finite element method.
- The applied fracture energy formulation works badly with irregular elements, see Sec. 2.6.
- Periodic boundary conditions are much easier to apply if opposite faces of the unit cell match.

For the determination of material properties four different load cases are considered, see Fig. 4. Loads were applied displacement driven, because force-driven load application fails beyond the point of maximum load. The necessary periodic boundary conditions are chosen according to [4], except for transverse shear. For each normal load case all unit cell faces are forced to stay even and parallel. The boundary conditions for shear loading are derived out of the transversely isotropic material symmetry of an UD-lamina. In-plane shear involves two different directions and is therefore modelled as simple shear. In contrast to [4] transverse shear is modelled as pure shear, because it involves two similar directions. For better understanding of the ongoing deformations under shear Fig. 5 shows the in-plane shear deformation of a hexagonal unit cell on the left and the transverse shear deformation of a square unit cell on the right. In the following only results for transverse compressive strain are shown, because the used material does not account for the highly nonlinear epoxy behavior under shear.

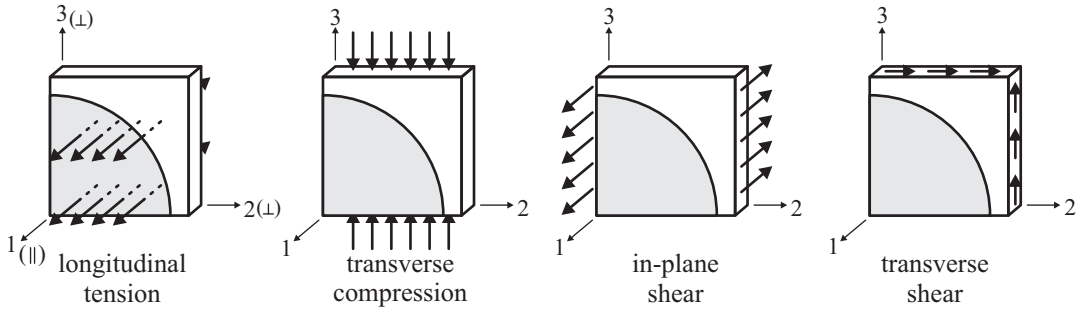

Figure 4: Different loading conditions

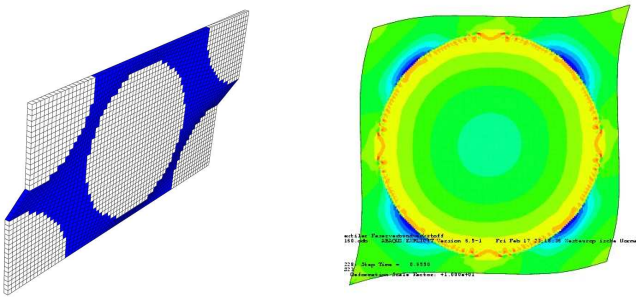

Figure 5: Deformations caused by in-plane shear (left) and transverse shear (right)

2.3 Transverse compressive strain

In the WWFE [3] the nonlinear behavior of UD-laminae under transverse compressive strain is given. These experimental results are compared to unit cell computations in Fig. 6. The most noticeable result is the difference between the stiffnesses of square and hexagonal arrangement. This has as well been observed in other publications [1][4] and will be discussed in detail in the next section. Both arrangements show good convergence due to the fracture energy approach.

Results for all load cases of Fig. 4 are summarized in table 2 for square and hexagonal arrangements. The test results are given in the WWFE [3]. Table 2 shows that the differences between square and hexagonal arrangements are quite considerable. Most notably the stiffness in transverse direction is predicted much better by the square arrangement, but it also overestimates the strength. It can be concluded that it altogether provides better results than the hexagonal arrangement.

Under in-plane shear the UD-lamina exhibits pronounced nonlinear behavior. Therefore further studies with a better description of the nonlinear behavior of the epoxy are planned. The given material parameters are obviously not sufficient for a reliable prediction in this load case. The applied unit cells are not capable of predicting fibre kinking under longitudinal compression. This phenomenon is massively influenced by fibre waviness and can only be analyzed with unit cells on a greater scale.

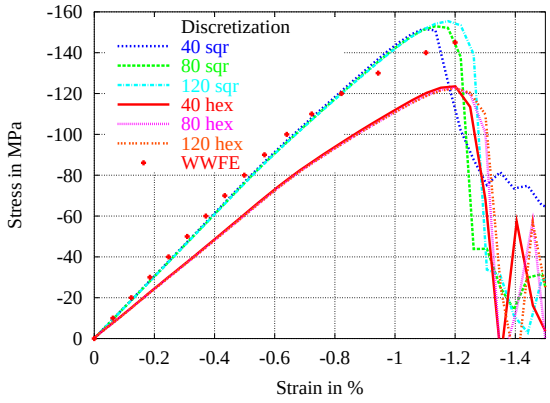

Figure 6: Stress-strain curves for different discretizations under transverse compressive strain compared to test results from WWFE

Table 2: Mechanical properties E-Glass MY750/HY917/DY063-epoxy lamina

Properties	Unit	Test results	Hexagonal	Square
Longitudinal modulus[1] $E_{\parallel}$	GPa	45.6	45,7	45,7
Longitudinal tensile strength $R^t_{\parallel}$	MPa	1280	1308	1308
Longitudinal tensile failure strain $\varepsilon^t_{\parallel}$	%	2.807	2.94	2.94
Transverse modulus[1] $E_{\perp}$	GPa	16.2	12.1	15.2
Transverse compressive strength $R^c_{\perp}$	MPa	145	122.9	156
Transverse compressive failure strain $\varepsilon^c_{\perp}$	%	1.2	1.2	1.18
In-plane Shear Modulus[1] $G_{\parallel\perp}$	GPa	5.83	4.43	4.68
In-plane Poisson's ratio $\upsilon_{\parallel\perp}$		0.278	0.251	0.249
In-plane Shear Strength $R_{\parallel\perp}$	MPa	73	–[2]	–[2]
In-plane Shear failure strain $\upsilon_{\parallel\perp u}$	%	4	–[2]	–[2]
Transverse Shear Modulus[1] $G_{\perp\perp}$	GPa	–	3.63	3.27
Transverse Poisson's ratio $\upsilon_{\perp\perp}$		0.4	0.39	0.26
Transverse Shear Strength $R_{\perp\perp}$	MPa	–	–[2]	–[2]
Transverse Shear failure strain $\upsilon_{\perp\perp u}$	%	–	–[2]	–[2]

[1] Initial modulus

[2] Still under investigation

2.4 Different stiffness of arrangements

Obviously the square arrangement is stiffer than the hexagonal arrangement. This can be easily understood when looking at the unit cells in Fig. 7. Both unit cells have the same fibre volume fraction of $V_f = 60\ \%$. For transverse compression fibre and matrix can be seen as series springs. The fibre is stiffer than the matrix by an order of magnitude, therefore the matrix is mainly responsible for the transverse stiffness. In the square arrangement the radius of the fibre is greater, i.e.

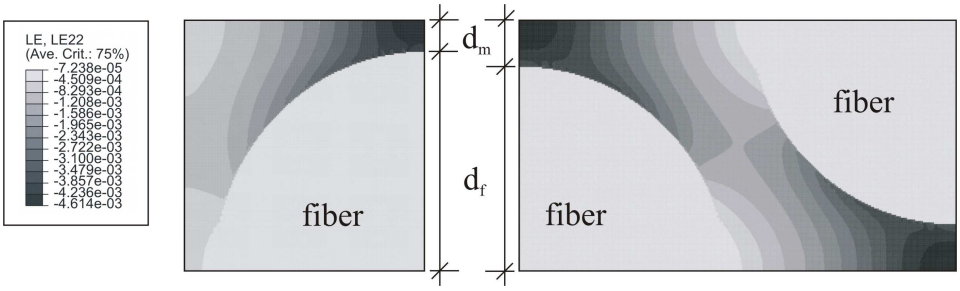

Figure 7: Strain distribution in square and hexagonal arrangement of unit cell

the proportion of the matrix d_m in load-direction is smaller. Hence the square-packed unit cell is stiffer than the hexagonal-packed unit cell. The strain distributions in Fig. 7 show the relevance of this fibre to matrix proportion.

If the aspect ratio of the unit cell is varied keeping the volume fraction constant, the stiffness of the unit cell changes according to Fig. 8. It is shown that the stiffness of the unit cell is mainly dependent on the ratio of the epoxy to the height of the cell $r_e = \frac{d_m}{d} = \frac{d_m}{d_m+d_f}$. For unit cells with a small ratio r_e there are almost no differences between hexagonal and square arrangement. With growing ratio r_e the results differ only slightly. Thus it must be concluded that the square arrangement is more suited to model an UD-lamina.

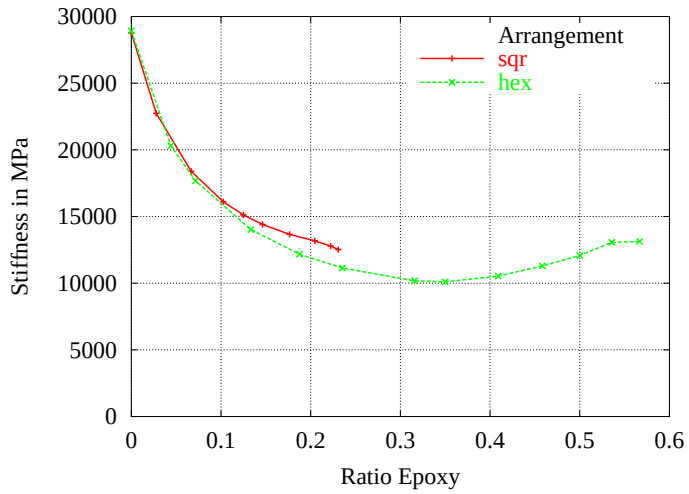

Figure 8: Stiffness of square and hexagonal unit cells after variation of aspect ratio

2.5 Influence of fracture energy

It may be argued that it is sufficient to determine failure of unit cells via the maximal stresses or strains of the matrix. The computational effort could easily be reduced by such an procedure, but, as Fig. 9 shows, it provides by far too conservative results. Fig.9 shows stress-strain curves for

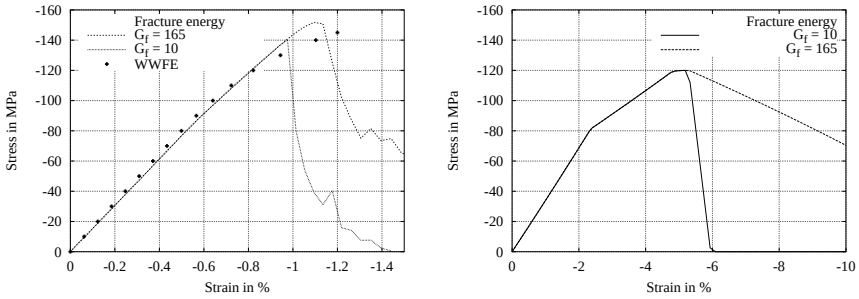

Figure 9: Influence of fracture energy on unit cell (left) and matrix material behavior (right)

different fracture energies. On the left side a stress-strain curve for a unit cell under transverse compressive strain and on the right the stress-strain curve of the epoxy matrix are shown. Using the measured fracture energy $G_f = 165\frac{J}{mm^2}$ yields a good agreement with experimental results, whereas $G_f = 10\frac{J}{mm^2}$, representing a brittle matrix, results in clearly too small failure stress and strain. A realistic fracture energy in the present case allows for load redistribution and thus realistic strength. Therefore it is very important to apply continuum damage mechanics in the strength computation of unit cell models.

2.6 Influence of irregular elements

In a conventional mesh the interface between fiber and matrix is modelled perfectly, see Fig. 10. Therefore irregular elements occur in the mesh that incur a mesh dependency as shown in Fig. 10. The characteristic length L ,see Sec. 2, of each element is the cubic root of its volume. This length is taken for each direction and multiplied with the strains, see Eq. 2, hence irregular elements degradate faster in one direction than in others. In Fig. 10 it can easily be seen that the irregular elements in the middle of the first mesh act as "crack-stoppers". In the second mesh all elements on the interface have an aspect ratio close to unity, thus the damage evolutes along the interface.

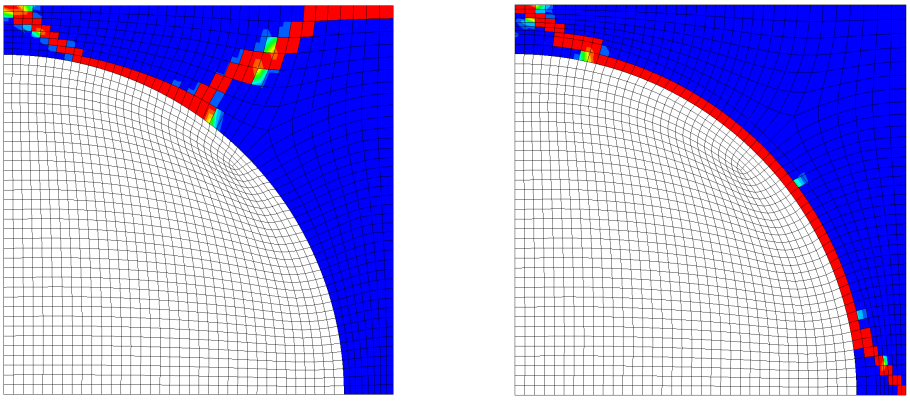

Figure 10: Damage evolution in conventional mesh dependent on mesh

Whilst for this rather simple geometry the mesh-dependency comes out clearly, it is already quite cumbersome to prevent it by manually generating regular elements in sensitive areas. For more complicated textile fiber geometries it is almost impossible to avoid irregular elements in sensitive areas. In the voxel mesh this kind of mesh dependency does not occur, therefore it is very apt for application together with the fracture energy approach.

3 Conclusion and outlook

An unit cell model has been introduced that shows a good capability for the strength prediction of UD-laminae. The fracture energy formulation provides a good convergence of results together with the voxel mesh. Significant differences in the results of square and hexagonal arrangement unit cells have been found. It has been shown that the consideration of the fracture energy is necessary for a realistic unit cell failure computation. The results of shear failure are hardly to determine without a good description of epoxy material. Under normal loading the proposed unit cells are able to provide a good prediction of failure.

Acknowledgements

Part of this work was funded by the German Research Council (DFG) within the framework of SPP-1123 *Textile composite design and manufacturing technologies for lightweight structures in mechanical and vehicle engineering* and by the German Academic Exchange Service (DAAD). This support is highly appreciated.

References

[1] Andrew J. Gunnion. *Analytical assessment of fibre misalignment in advanced composite materials*. PhD thesis, RMIT University, Melbourne, 2004.

[2] A. Hillerborg, M. Modeer, and P. E. Petersson. Analysis of crack formation and crack growth in concrete by means of fracture mechanics and finite elements. *Cement and Concrete Research*, 6:773–782, 1976.

[3] M.J.Hinton, A.S. Kaddour, and P.D. Soden, editors. *Failure criteria in fibre reinforced polymer composites: The World-Wide Failure Exercise*. Elsevier Science, Oxford, 2004.

[4] C. T. Sun and R. S. Vaidya. Prediction of composite properties from a representative volume element. *Composites Science und Technology*, 56:171–179, 1996.